Treadmilling stability of a one-dimensional actin growth model

Rohan C. Abeyaratne[a], Eric Puntel[b,*], Giuseppe Tomassetti[c]

[a] *Department of Mechanical Engineering, Massachusetts Institute of Technology, Cambridge, MA, USA*
[b] *Dipartimento Politecnico di Ingegneria e Architettura, Università di Udine, via del Cotonificio 114, Udine I-33100, Italy*
[c] *Dipartimento di Ingegneria, Università degli Studi Roma Tre, via Volterra 62, Roma I-00146, Italy*

Abstract

Actin growth is a fundamental biophysical process and it is, at the same time, a prototypical example of diffusion-mediated surface growth. We formulate a coupled chemo-mechanical, one-dimensional growth model encompassing both material accretion and ablation. A rod-like element composed of actin monomers is fixed at one end and connected to an elastic device at the other. The mechanical behaviour of the rod, the diffusion of free actin monomers in a surrounding solvent and the kinetic growth laws at the accreting/ablating ends are accounted for. The constitutive behaviour of actin is prescribed in fairly general terms by mainly requiring that the elastic strain energy density of the material be convex. Treadmilling solutions, characterized by a constant length of the continuously evolving body, are investigated. Existence and stability results are condensed in the form of simple formulas and discussed.

Keywords: actin, treadmilling, stability, surface growth

sec:intro

1. Introduction

It is well known that growth in living systems is not only promoted by biological and chemical signals but results as well from mechanical stimuli (Goriely, 2017).

Modelling growth, intended as variation of mass, poses a number of challenges in mechanics which are still being actively investigated. Among them is surface growth or accretion which, following the work of Skalak and others (Skalak et al., 1982, 1997), requires to define and track in time an ever changing, usually stress-free, reference configuration, i.e. collection of material points. The

*Corresponding Author.
Email addresses: rohan@mit.edu (Rohan C. Abeyaratne), eric.puntel@uniud.it (Eric Puntel), giuseppe.tomassetti@uniroma3.it (Giuseppe Tomassetti)

phenomenon of accretion of a solid on its boundary, occurs in several contexts of physical, technological, and biological interest. One of the most common examples of surface growth is the solidification of water at the ice-water interface near the freezing temperature; other examples include technological processes such as chemical vapor deposition, 3D printing and layered building (Bacigalupo and Gambarotta, 2012; Zurlo and Truskinovsky, 2017, 2018); in biology, the growth of hard tissues like bones and teeth (Ciarletta et al., 2013; Ganghoffer and Goda, 2018).

A second delicate issue regards the prescription of a growth law. One may simply assume that as given. Conversely, growth speed could be obtained as a result of mechanical and biochemical local conditions. These in turn may be expressed by a suitable kinetic law once the thermodynamical force driving growth is consistently defined (Abeyaratne and Knowles, 1990; Tomassetti et al., 2016).

Third, one may also describe the transport of free particles providing the material constituents for growth. In this way essential features of growth may emerge from the balance of tied mechanical and biochemical responses.

In this work we precisely analyze a one-dimensional model featuring the three aforementioned characteristics, albeit in a simplified manner. We consider an elastic bar fixed at one end and connected to an elastic device at the other. The bar can grow by attaching or detaching its constituting particles (or monomers), at either end. The diffusion of free particles in a surrounding or permeating solvent and the kinetic condition for growth are accounted for. The first objective of this model is to investigate a basic reference template of chemo-mechanical growth which allows to discuss more easily modelling choices, notions and solutions.

The second motivation for this study is provided by a specific biological example, namely the growth of actin filaments. Actin in its polymerized network-forming state is an essential constituent of the cytoskeleton and is involved in cell contraction, division, motility. It is intensely studied in the bio-physical literature. See e.g. Prost et al. (2015) for a review on the physics of active gels like actin, the Ph.D. thesis of Zimmermann (2014) for a review of quantitative models of actin-based motility, and Bindschadler et al. (2004) and Cardamone et al. (2011) for just two of the many examples of different biophysical and computational models of the properties of actin networks. Pertinent to this study, but not including mechanical aspects, is a one-dimensional mathematical model of actin polymerization kinetics by Edelstein-Keshet and Ermentrout (2000).

There are interesting experimental studies (Parekh et al., 2005; Chaudhuri et al., 2007; Bieling et al., 2016) which have a setup similar to the one considered herein: an actin network is grown on a surface below the cantilever tip of an atomic force microscope (AFM) thus realizing a rod-like structure fixed at one end and restrained by an elastic device at the other. Among other things, these experiments consistently suggest that the actin network adapts to higher values of applied compressive force by correspondingly increasing its density and stiffness. This is a feature that is currently not included in our model, but it constitutes a possible refinement for future work.

Actin filaments exhibit a peculiar growth mode called treadmilling in which the length of the filament remains constant while accreting (i.e. adding) actin monomers at one end and ablating (i.e. shedding) them at the other at equal rates (see e.g. Theriot, 2000). This energy dissipating state is made possible by the hydrolysis of ATP (adenosine triphosphate) bound to actin monomers into an ADP (adenosine diphosphate) molecule and a phosphate. Despite its peculiarity, treadmilling may also be seen as a specific instance of a more common biological paradigm by which systems, tissues or organisms continuously substitute their constituents or cells at specific rates even when their overall size is no longer changing.

This work has two main results. First, under general assumptions on the behaviour of the material constituting the bar, it is possible to condense in simple formulas conditions for the existence of treadmilling states.

Secondly the stability of such solutions is discussed. Herein stability is not addressed geometrically in classical structural mechanics terms (i.e. buckling) but rather dynamically, asking whether perturbations of the treadmilling state may cause the bar to abandon indefinitely its stationary length. For the treadmilling case in which ATP molecules accrete at the fixed end of the bar, it is possible to prove global stability under arbitrary initial conditions.

These results can hopefully constitute a useful term of comparison and interpretative tool for other more complex models and experiments. For instance, the latter one concerning global stability of a treadmilling solution may provide clarification or further evidence in support of the "emergence of a universal growth path" observed in a similar context by Abi-Akl et al. (2019).

The discussion on stability of the solution has also been motivated by experiments studying the growth and relative stability of an annulus of actin accreting on the surface of a spherical bead (Cameron et al., 1999; Noireaux et al., 2000; van der Gucht et al., 2005). These experiments where in turn inspired by bacterium Listeria monocytogenes which exploits cytoplasmic actin to form a polymerized tail and move out of the cell membrane and spread (Prost et al., 2008). Existing numerical and modelling efforts on this subject can be found in (John et al., 2008; de Buyl et al., 2013).

A model for a spherical annulus of actin growing on the surface of a sphere was formulated by Tomassetti et al. (2016). Therein the treadmilling solutions were characterized as well. A planned continuation of the above study and of the present one is the analysis of stability of the treadmilling solutions of that system. Other extension of the present work include accounting for the aforementioned dependence of actin stiffness and density on externally applied stress and deriving analytical relationships between growth velocity and external force to be compared with experimental ones.

The article is structured as follows. Section 2 describes the one-dimensional model in its mechanical, chemical and growth aspects. Section 3 provides the material constitutive description of the bar while the derivation of the kinetic laws is given in Section 4. The system is reduced to a differential algebraic equation in Section 5, a form suitable for the discussion concerning the existence and stability of treadmilling solutions carried out in Section 6. Conclusive remarks

are made in Section 7.

sec:model

2. One-dimensional model

ss:set

2.1. *Problem setting*

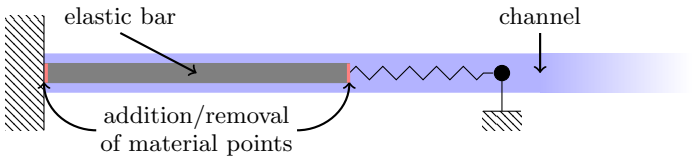

Figure 1: An elastic bar clamped between a hard and a soft device, immersed in a semi-infinite channel.

fig:setup

We consider a one-dimensional body, represented by a bar in Figure 1, which grows and deforms in a one-dimensional physical space.

The bar has a natural reference configuration that occupies the segment $(x_0(t), x_1(t))$ and whose generic point is denoted by x . Here and in the following subscripts 0 and 1 refer to the left and right end sections of the bar respectively, both in the reference and in the current configurations.

As represented in Figure 2, the body is mapped into (?) the physical one-dimensional space through the function $y(x,t)$ where it occupies the segment $(y_0(t), y_1(t))$. Here and in what follows the shorthand notation

$$f_\alpha(t) = f(x_\alpha(t), t) \qquad \text{with } \alpha = 0, 1 \ , \tag{1}$$

eq:fam

denotes in general the value of a material quantity $f(x,t)$ at the end sections of the bar at time t. In particular $y_0(t)$ and $y_1(t)$ simply indicate the position of the end sections of the bar in the current configuration.

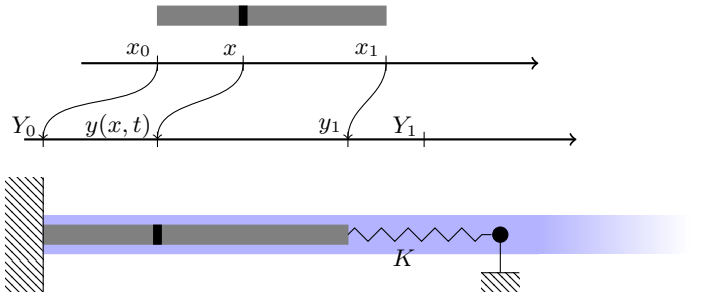

Figure 2: Reference (top) and current (bottom) configuration of the elastic bar.

fig:onedim

In regard to constraints, the terminal side x_0 of the bar is attached to the point Y_0 in the physical space, so that $y_0 = y(x_0(t), t) = Y_0$. Likewise, the

terminal side x_1 is attached to one end of a linear spring of stiffness K. The rest position of this end of the spring is Y_1, i.e. the spring is unstretched with zero force when this end is at Y_1. Its other end is fixed. It is worth noting that while the left-hand end of the bar is always located at Y_0 in physical space, the right-hand end is located at Y_1 only when the spring force vanishes.

The bar is made of "material units", hereafter referred to as *monomers*, which are in a bound, polymerized state. The same monomers in a free, unbound state are in solution in the solvent which fills a one dimensional infinite channel, depicted with a blue-shaded rectangle in Figure 1. Free monomers flow in the interval $(y_0(t), y_1(t)) = (Y_0, y_1(t))$ according to Fick's law. We can think of them as either flowing only through the bar or flowing as well through the portion of the channel not occupied by the bar. They can freely cross the point y_1, where the body is in contact with a reservoir of monomers, but cannot flow past the left support $y_0 = Y_0$ which is assumed to be impermeable. The chemical potential μ_1 of free monomers at $y_1(t)$ is held fixed and equal to M_1 , and there is an infinite supply of monomers at y_1.

I tried consistently using capital letters Y,M for prescribed values, small case for fields y,μ, and subscripts y_α,μ_α for values of the fields at the end cross sections.

Finally, under suitable growth conditions to be later specified, free monomers may accrete, i.e. attach, at either end of the bar and conversely, bound monomers occupying the end positions x_0 and x_1 of the bar may ablate, i.e. detach, and return to their free state. When accretion or ablation occurs, the referential points x_0 and x_1, and hence the reference length of the bar, can change. Specifically, at the left-hand end x_0, accretion occurs when $\dot{x}_0 < 0$ while ablation occurs when $\dot{x}_0 > 0$. Similarly accretion and ablation at the right-hand end x_1 correspond to $\dot{x}_1 > 0$ and $\dot{x}_1 < 0$ respectively.

We now specify the equations governing the system just described.

ss:mech

2.2. Mechanics

We require the deformation mapping $y(x,t) : x \to y$ to be one to one by prescribing that the stretch $\lambda = y' = \partial y/\partial x$ be positive:

$$\lambda(x,t) = y'(x,t) > 0 \ .$$

Here and in the following we use the prime to denote the derivative with respect to a variable other than time. That is $f' = \partial f/\partial \bullet$ with $f = f(\bullet)$ or $f = f(\bullet, t)$ with t indicating time and $\bullet \neq t$. The dot is used, as customary, to indicate partial derivative with respect to time, i.e. $\dot{f} = \partial f/\partial t$.

We assume the material to be hyperelastic and therefore characterized by a convex strain energy density $W(\lambda)$ from which we can compute the axial force σ in the bar as

$$\sigma(x,t) = W'(\lambda(x,t)) \ .$$

A number of additional assumptions on the strain energy density are detailed in Section 3.1. Given that W does not depend explicitly on x, the material constituting the bar is taken to be homogeneous.

The mechanical model for the bar is summarized in the set of equations (2) below.

eq:mech

$$\begin{cases} \dfrac{\partial \sigma}{\partial x} = 0 & \text{in } (x_0(t), x_1(t)), \quad (2a) \\ \sigma = W'(\lambda), \quad \lambda = y' & \text{in } (x_0(t), x_1(t)), \quad (2b) \\ y_0(t) = y(x_0(t), t) = Y_0 & \text{in } x_0(t), \quad (2c) \\ \sigma_1(t) + K(y_1(t) - Y_1) = 0 & \text{in } x_1(t)\ . \quad (2d) \end{cases}$$

eq:mech1 eq:mech2 eq:mech3 eq:mech4

Equation (2a) represents local equilibrium in the reference configuration and implies that the axial force is constant in x. In eq. (2b) we state again the constitutive law and the definition of the stretch λ. Being σ constant in x, it follows that λ is constant in x and that y is linear in x.

The boundary condition prescribing that the leftmost section of the bar is fixed in $y = Y_0$ is expressed in eq. (2c). The axial force $\sigma_1(t) = \sigma(x_1(t), t)$ in the bar at $x = x_1(t)$ is prescribed by the force in the spring of stiffness K in eq. (2d). Since σ is independent of x, (2d) actually prescribes the value of the axial force in the whole bar.

ss:diff eq:diff

2.3. Diffusion

The following system

$$\begin{cases} \dfrac{\partial h}{\partial y} = 0 & \text{in } (Y_0, y_1(t)), \quad (3a) \\ h + m\mu' = 0 & \text{in } (Y_0, y_1(t)), \quad (3b) \\ h(y_0(t), t) = h(Y_0, t) = \varrho \dot{x}_0(t) & \text{in } Y_0, \quad (3c) \\ \mu(y_1(t), t) = M_1 & \text{in } y_1(t)\ . \quad (3d) \end{cases}$$

eq:diff1 eq:diff2 eq:diff3 eq:diff4

governs the flux of free monomers in the solvent. Here $h(y, t)$ is the monomer flux in the positive y direction, $\mu(y, t)$ is the associated chemical potential and m is the mobility. The first equation (3a) expresses the conservation of mass. In it we have omitted a term $\partial h/\partial t$ by assuming that diffusion is much faster than growth. Flux has the dimension of moles per unit time. The second equation (3b) represents Fick's law. The third equation (3c), a boundary balance of mass, states that the flux of monomers at the impermeable wall is equal to the amount of monomers that detach from the left endpoint of the bar per unit time, which in turn is proportional to the ablation velocity $\dot{x}_0$ through a constant ϱ. We think of ϱ as the number of moles of bound actin monomer per unit length in the reference configuration. The fourth equation (3d) expresses the condition of chemical equilibrium at y_1 by equating $\mu_1 = \mu(y_1(t), t)$ to the chemical potential M_1 of the monomers in the semi-infinite monomer pool to the right of y_1. Note that $\mu_0 = \mu(y_0, t)$ is as yet unknown and to be determined.

We could use the prime in (2a) and (3a) if you prefer. I did not use it because I wanted to highlight the dependence on x and y respectively.

If we use μ_0 for $\mu(y_0, t)$, I am uncomfortable using μ_1 for both $\mu(y_1, t)$ and M_1. Should we extend the notation defined in eq. (1)?

ss:accr

2.4. Accretion

As anticipated in the Introduction, a key ingredient of this model is the growth law governing the evolution of the referential configuration of the bar. We assume a simple, linear kinetic law of the form

$$B_\alpha V_\alpha = F_\alpha \qquad \text{with } \alpha = 0, 1 \qquad (4)$$

eq:kinshort

In eq. (4), $\alpha = 0, 1$ refer to the ends of the bar, V_α is the accretion velocity, B_α is a positive kinetic coefficient and F_α is the thermodynamical force driving accretion. Note that $V_0 = -\dot{x}_0$ and $V_1 = \dot{x}_1$. Realistically (4) is most suitable for small deviations from thermodynamic equilibrium. The expression for F_α, derived afterwards in Section 4, is

$$F_\alpha = \varrho(\mu_\alpha - M_{B,\alpha}) + W^*(\sigma_\alpha), \tag{5}$$

eq:Fa

where σ_α and μ_α are *material* descriptions of the fields μ, σ evaluated at x_α following the notation introduced in (1). Parameter $M_{B,\alpha}$ is a material constant interpreted as the chemical potential of *bound* monomers at x_α and $W^*(\sigma)$ is the *complementary* strain energy density whose definition and properties are given in Section 3.2. In particular in there we will see that a tensile force $\sigma > 0$ corresponds to positive $W^*(\sigma)$ thus promoting growth according to (4)-(5). This is consistent with the layman's notion of stress induced growth popularized by images of abnormal growth of earlobes, necks and other body parts subject to sustained tension, especially observed in some indigenous tribes (see e.g. Goriely, 2017, Chapter 2.1).

Motivated by the behaviour of actin filaments, see e.g. Theriot (2000) or Alberts et al. (2015, panel 16-2), we admit two distinct values $M_{B,0}$ and $M_{B,1}$ for the chemical potential of monomers in the bound state. Actin monomers are bound to ATP (Adenosine TriPhosphate) when they first polymerize, i.e. accrete, but after some time a hydrolysis reaction ensues by which the ATP releases a phosphate group and the polymerized actin monomer is now tied to an ADP (Adenosine DiPhosphate) molecule. The hydrolysis reaction releases energy, part of which remains stored in the polymerized actin (Rohan's comment: I don't understand this. On one hand it is released, on the other it is stored? $\longrightarrow$ see Alberts et al. (2015), page 901). Therefore ADP-actin is at a higher energy level, i.e. chemical potential, than ATP-actin. Due to differences in the properties of opposite ends of actin filaments, one end may be occupied by a lower-energy ATP-actin monomer and the other by a higher energy ADP bound actin monomer. Hence the distinction between values of the chemical potential of polymerized actin $M_{B,0}$ and $M_{B,1}$ at the two ends of the bar.

removed, "barbed" and "pointed", but not added inequality $M_{B,0}$ smaller than $M_{B,1}$

As noted previously, a positive accretion velocity corresponds to a negative rate $\dot{x}_0$ and to a positive rate $\dot{x}_1$ whence $V_0 = -\dot{x}_0$ and $V_1 = \dot{x}_1$, and recalling that we are using the notation of equation (1), the specialization of (4) and (5) to the two ends of the bar can be written as

eq:accr

$$\begin{cases} -B_0\dot{x}_0(t) = \varrho(\mu_0 - M_{B,0}) + W^*(\sigma_0(t)) \,, & \text{(6a)} \\ \quad B_1\dot{x}_1(t) = \varrho(\mu_1 - M_{B,1}) + W^*(\sigma_1(t)) \,. & \text{(6b)} \end{cases}$$

eq:accr1 eq:accr2

Despite the simplicity of the one-dimensional model, the above equations close the feedback loop between stress and growth. On the one hand, the presence of the spring in (2) allows growth to affect stress, while on the other hand, growth rates in (6) are influenced by stress.

The evolution equations (6) also provide closure for the boundary-value problem (2) and (3). In fact, the solution of (2)–(3) depends only on the instan-

taneous values of $x_0(t)$, $x_1(t)$ and of the rate $\dot{x}_0(t)$. This means, in particular, that the right-hand sides of the equations (6) ultimately depend only on $x_0(t)$, $x_1(t)$ and $\dot{x}_0(t)$. We therefore conclude that the combination of (2), (3), and (6) is equivalent to a first-order system in the unknowns $x_0(t)$ and $x_1(t)$. As such, this system must be complemented by initial conditions

$$x_0(0) = x_{00}, \qquad x_1(0) = x_{10} \quad \text{and} \quad y_0(0) = Y_{00} = Y_0, \qquad y_1(0) = Y_{10}. \tag{7}$$ eq:xyinit

sec:const

3. Constitutive behaviour

We assume the bar to be made of a homogeneous, hyperelastic material and we define its constitutive behaviour through the strain energy density function $W(\lambda)$. As seen in equation (2b), the force σ is given by $W'(\lambda)$ while $W''(\lambda)$ represents the tangent stiffness.

ss:W

3.1. Strain energy density

eq:Wass

A specific expression for $W(\lambda)$ is not prescribed. Instead, we merely assume that the strain energy density has the following characteristics:

$$\begin{cases} W(1) = 0 & & \text{(8a)} & \texttt{eq:Wass1} \\ W'(1) = 0 & & \text{(8b)} & \texttt{eq:Wass2} \\ W(\lambda) \to +\infty & \text{as } \lambda \to 0^+ & \text{(8c)} & \texttt{eq:Wass3} \\ W(\lambda) \to +\infty & \text{as } \lambda \to +\infty & \text{(8d)} & \texttt{eq:Wass4} \\ W'(\lambda) \to +\infty & \text{as } \lambda \to +\infty & \text{(8e)} & \texttt{eq:Wass5} \\ W''(\lambda) > 0 & \forall \lambda > 0 & \text{(8f)} & \texttt{eq:Wass6} \end{cases}$$

discussed in the following.

The strain energy density is defined but for an arbitrary constant which is conveniently set in (8a) by assigning zero energy to the undeformed state in which the stretch λ is equal to 1. In this latter case the force σ is also zero according to eq. (8b). Equations (8c) and (8d) express the requirement that infinite strain energy is necessary to, respectively, infinitely compress and infinitely extend the material. Probably the strongest condition on $W(\lambda)$ is given by eq. (8f) which enforces convexity of the strain energy which in turn implies that the stress is a monotonic function of the stretch, and the tangent stiffness is positive everywhere, i.e. there are no stress softening branches under increasing stretch. Note that $\sigma > 0$ for $\lambda > 1$ and $\sigma < 0$ for $0 < \lambda < 1$. Assuming sufficient regularity of $W(\lambda)$, equations (8c) and (8f) can be used to prove that, when the stretch tends to zero, the force tends to infinity, that is $\sigma \to -\infty$ when $\lambda \to 0^+$. It is easy to see that conditions (8d) and (8f) are not sufficient to obtain an analogous result for the case in which the stretch tends to infinity. The condition that $\sigma \to +\infty$ when $\lambda \to +\infty$ is therefore explicitly given in (8e). We note in passing that the set of assumptions (8) is introduced in a constructive way and is not minimal since (8d) follows from (8e) and (8f).

From the properties of $W(\lambda)$ ensue those of the force σ. Let

$$\widehat{\sigma}(\lambda) := W'(\lambda) \quad , \quad \widehat{\sigma}(\lambda) : \mathbb{R}^+ \longrightarrow \mathbb{R} \, . \tag{9}$$ eq:shat

Then from (8f) we know that $\widehat{\sigma}$ is monotonically increasing and, taking into account (8c)-(8e) as well, that it spans the whole real line.

The force $\widehat{\sigma}$ as a function of the stretch is therefore invertible and function

$$\widehat{\lambda}(\sigma) : \mathbb{R} \longrightarrow \mathbb{R}^+ \, , \quad \widehat{\lambda}(\sigma) \text{ such that } W'(\widehat{\lambda}) = \sigma \tag{10}$$ eq:lhat

is uniquely defined. It can be easily seen that $\widehat{\lambda}(\sigma)$ is monotonically increasing

$$\widehat{\lambda}'(\sigma) = \frac{1}{W''(\lambda)} > 0 \tag{11}$$ eq:lhat'

and that it possesses the following properties:

$$\widehat{\lambda}(\sigma) \to 0^+ \text{ as } \sigma \to -\infty, \qquad \widehat{\lambda}(0) = 1, \qquad \widehat{\lambda}(\sigma) \to +\infty \text{ as } \sigma \to +\infty. \tag{12}$$ eq:lhatprop

ss:W*

3.2. Complementary strain energy density

The complementary strain energy density $W^*(\sigma)$ is the Legendre transform of $W(\lambda)$. It defined as

$$W^*(\sigma) = \sigma\widehat{\lambda}(\sigma) - W(\widehat{\lambda}(\sigma)) \, , \tag{13}$$ eq:W*def

eq:W*

and has the properties

$$\begin{cases} W^{*\,\prime}(\sigma) = \lambda > 0 & \text{with } \lambda = \widehat{\lambda}(\sigma) \quad (14a) \quad \texttt{eq:W*1} \\ W^{*\,\prime\prime}(\sigma) = \widehat{\lambda}'(\sigma) > 0 & \forall \sigma \in \mathbb{R} \quad (14b) \quad \texttt{eq:W*2} \\ W^{*\,\prime}(\sigma) \to 0^+ & \text{as } \sigma \to -\infty \quad (14c) \quad \texttt{eq:W*3} \\ W^{*\,\prime}(\sigma) \to +\infty & \text{as } \sigma \to +\infty \quad (14d) \quad \texttt{eq:W*4} \\ W^*(0) = 0 & \quad (14e) \quad \texttt{eq:W*5} \\ W^*(\sigma) \to \pm\infty & \text{as } \sigma \to \pm\infty \quad (14f) \quad \texttt{eq:W*6} \end{cases}$$

all of which follow from assumptions we have made previously. The key property of $W^*(\sigma)$ is (14a). It ensues from the definition (13) since

$$W^{*\,\prime}(\sigma) = \widehat{\lambda}(\sigma) + \sigma\widehat{\lambda}'(\sigma) - W'(\lambda)\widehat{\lambda}'(\sigma) = \widehat{\lambda}(\sigma) \, .$$

Given that λ is always positive, we have that $W^*(\sigma)$ is a monotonically increasing function. Moreover, (14b) follows from (11) whence $W^*(\sigma)$ is also strictly convex. Properties (14c) and (14d) are simply restatements of (12). Property (14e) follows from the definition of $W^*(\sigma)$ and, together with monotonicity, implies that $W^*(\sigma) > 0$ when $\sigma > 0$ and $W^*(\sigma) < 0$ when $\sigma < 0$. The last property (14f) follows as well from the definition and the preceding properties. It is important because it implies that $W^*(\sigma) : \mathbb{R} \longrightarrow \mathbb{R}$ is surjective, and given the injectivity implied by (14a), also invertible. We will use this result in what follows, so it is worth noticing that it is a consequence of the assumptions (8c) and (8e).

ss:Wex

3.3. Examples of strain energy densities

We provide here a couple of instances of strain energy densities satisfying the requirements in eq. (8). We add also some remarks on the asymptotic growth of the constitutive laws $\widehat{\sigma}(\lambda)$ and complementary strain energy densities W^* ensuing from choices of the asymptotic dominant term of the strain energy density W.

Adding the examples in order to use them for figures

A rational function

First let's consider an example of a rational strain energy density:

$$W(\lambda) = \frac{EA}{6}(\lambda^2 + 2\lambda^{-1} - 3)\,, \tag{15}$$

eq:Wex1

whence $\sigma = W'(\lambda) = \frac{EA}{3}(\lambda - \lambda^{-2})$ and $W''(\lambda) = \frac{EA}{3}(1 + 2\lambda^{-3})$. Notice that $W''(1) = EA$ and that this W obeys all assumptions in (8). Then W^* can be obtained,

$$W^* = \frac{EA}{6}\left[\lambda^2 - 4\lambda^{-1} + 3\right]\Big|_{\lambda=\widehat{\lambda}(\sigma)}\,,$$

together with its derivatives,

$$W^{*\prime}(\sigma) = \lambda\Big|_{\lambda=\widehat{\lambda}(\sigma)} > 0 \quad \text{and} \quad W^{*\prime\prime}(\sigma) = \frac{3}{EA(1+2\lambda^{-3})}\Big|_{\lambda=\widehat{\lambda}(\sigma)} > 0\,.$$

The closed form expression of W^* is cumbersome, but we can easily look at its asymptotic behaviour when $\sigma \to \pm\infty$

$$W^* \sim \frac{3}{2}\frac{\sigma^2}{EA} \to +\infty \quad \text{for } \sigma \to +\infty, \qquad W^* \sim \sqrt{\frac{4}{3}EA}\,\sqrt{-\sigma} \to -\infty \quad \text{for } \sigma \to -\infty$$

More generally, suppose

$$W(\lambda) \sim \alpha\lambda^n, \qquad \sigma \sim \alpha n\lambda^{n-1}, \qquad \alpha > 0, n > 1, \qquad \text{as } \lambda \to \infty.$$

Then

$$\lambda \sim \left(\frac{\sigma}{\alpha n}\right)^{\frac{1}{n-1}}, \qquad W^* \sim \alpha(n-1)\left(\frac{\sigma}{\alpha n}\right)^{\frac{n}{n-1}} \to +\infty \qquad \text{as } \sigma \to +\infty.$$

Similarly suppose

$$W(\lambda) \sim \beta\lambda^{-m}, \qquad \sigma \sim -\beta m\lambda^{-m-1}, \qquad \beta > 0, m > 0, \qquad \text{as } \lambda \to 0.$$

Then

$$\lambda \sim \left(\frac{\beta m}{-\sigma}\right)^{\frac{1}{m+1}}, \qquad W^* \sim -\beta(m+1)\left(\frac{-\sigma}{\beta m}\right)^{\frac{m}{m+1}} \to -\infty \qquad \text{as } \sigma \to -\infty$$

A closed form expression

Choosing a strain energy density of the form

$$W(\lambda) = \frac{EA}{2}\left(\frac{\lambda^2}{2} - \ln\lambda - \frac{1}{2}\right), \qquad \sigma = W'(\lambda) = \frac{EA}{2}\left(\lambda - \lambda^{-1}\right)$$

it is possible to obtain in closed form

$$\widehat{\lambda}(\sigma) = \frac{\sigma}{EA} + \sqrt{\frac{\sigma^2}{(EA)^2} + 1}\,; \quad W^*(\sigma) = \frac{EA}{2}\left(\frac{\widehat{\lambda}^2(\sigma)}{2} + \ln\widehat{\lambda}(\sigma) - \frac{1}{2}\right). \tag{16}$$

eq:W*ex2

Also in this case we have that $W''(1) = EA$ and that W satisfies all requirements in (8).

sec:kinder

4. Derivation of the driving force

Accretion is a non-equilibrium process involving dissipation. The latter can be computed as the product of a flux, accretion rates in our case, and of a conjugate driving force which quantifies the departure from thermodynamic equilibrium.

In this section we provide the derivation of the expression of the driving force in eq. (5). We follow Tomassetti et al. (2016) and Abeyaratne and Knowles (1990, 1997).

We start from the expression of the dissipation rate associated with the bar,

$$\text{dissipation rate} \coloneqq \sigma\frac{dy}{dt}\Big|_{x_0}^{x_1} + \varrho(\mu - M_B)\dot{x}\Big|_{x_0}^{x_1} - \frac{d}{dt}\int_{x_0}^{x_1} W(\lambda)dx\,, \tag{17}$$

eq:dissdef

which is given by the sum of three terms. The first represents the mechanical power of external loads, the second the inflow of chemical energy per unit time and the third the energy flow per unit time elastically stored in the material and therefore not dissipated.

We observe that the velocity of a point on the boundary is given by

$$\dot{y}_\alpha(t) = \frac{d}{dt}y(x_\alpha(t), t) = v_\alpha + y'\dot{x}_\alpha = v_\alpha + \lambda_\alpha\dot{x}_\alpha, \tag{18}$$

eq:vel

from which we see that it is distinct from the velocity v_α of a material point sitting at the boundary at the current instant; here $v_\alpha(t) = v(x_\alpha(t), t)$ where $v(x,t) = \partial y(x,t)/\partial t$.

We rewrite the third term in (17) using Leibnitz's rule (the divergence theorem in one-dimension), transport theorems and equations (2a) and (2b),

$$\begin{aligned}\frac{d}{dt}\int_{x_0}^{x_1} W(\lambda)dx &= \int_{x_0}^{x_1} W'(\lambda)(\dot{y})'dx + W(\lambda)\dot{x}\Big|_{x_0}^{x_1} \\ &= (\sigma\dot{y} + W(\lambda))\dot{x}\Big|_{x_0}^{x_1}.\end{aligned} \tag{19}$$

eq:Wdiv

On substituting equations (18) and (19) into the expression (17) of the dissipation rate we obtain

$$\begin{aligned}\text{dissipation rate} &= (\sigma\dot{y} + \sigma\lambda\dot{x} + \varrho(\mu - M_B)\dot{x} - (\sigma\dot{y} + W(\lambda))\dot{x})\Big|_{x_0}^{x_1} \\ &= (\varrho(\mu - M_B) + (\sigma\lambda - W(\lambda)))\ \dot{x}\Big|_{x_0}^{x_1} \qquad (20) \quad \texttt{eq:diss2} \\ &= \Big(\varrho(\mu - M_B) + W^*(\sigma)\Big)\dot{x}\Big|_{x_0}^{x_1},\end{aligned}$$

in which the multiplier of the accretive flux $\dot{x}$ is precisely the driving force of growth introduced in equation (5).

sec:DAE

5. Reduction to a differential algebraic equation

Here the system of equations presented in Section 2 is reduced to a differential algebraic equation and new notation is introduced, suitable for the ensuing discussion on the existence and stability of treadmilling solutions.

ss:DAEmech

5.1. Mechanics

Let

$$\ell(t) = x_1(t) - x_0(t) > 0\,, \qquad (21) \quad \texttt{eq:ell}$$

be the length of the bar in the reference configuration. The integration of the mechanical system of equations (2) yields

eq:msol

$$\begin{cases} y(x,t) = \lambda(t)(x - x_0(t)) + Y_0, & \forall\ x_0(t) \le x \le x_1(t) \qquad (22a) \quad \texttt{eq:msol1} \\ \sigma(t) = W'(\lambda(t)) \qquad (22b) \quad \texttt{eq:msol2} \\ K\lambda(t)\ell(t) = \sigma_{\max} - \sigma(t) \qquad (22c) \quad \texttt{eq:msol3} \end{cases}$$

where we have termed

$$\sigma_{\max} = K(Y_1 - Y_0) \qquad (23) \quad \texttt{eq:smaxdef}$$

the maximum force attainable in the bar and in the spring. Since both $\lambda > 0$ and $\ell > 0$, it follows from (22c) that

$$\sigma < \sigma_{\max}. \qquad (24) \quad \texttt{eq:s<smax}$$

We consider $\sigma_{\max}$ to be an arbitrarily tunable parameter since we can imagine being able to vary the rest position Y_1 of the spring, to the right or to the left of Y_0, to attain any desired value of $\sigma_{\max}$.

From (22a) we have

$$\lambda = (y_1 - y_0)/(x_1 - x_0) = (y_1 - y_0)/\ell \qquad \Rightarrow \qquad (y_1 - y_0) = \lambda\ell \qquad (25) \quad \texttt{eq:lamell}$$

and so, as expected, $\lambda\ell$ denotes the length of the body in physical space.

Equations (22) describe a unique motion $y(x,t)$ and force $\sigma(t)$ in terms of x_0, x_1. To see it, combine (22b) and (22c) to give

$$W'(\lambda) = \sigma_{\max} - K\ell\lambda \tag{26}$$ eq:lamsol

In light of the assumed properties (8) of $W(\lambda)$, it is readily shown that there exists a unique root $\lambda > 0$ of this equation corresponding to any given $\ell > 0$, $K > 0$ and $\sigma_{\max}$. Moreover in view of (8f), the root λ decreases monotonically with increasing ℓ. The corresponding force is then given by (22b). These representations will of course involve given values of K, Y_0, Y_1 and the yet to be found values x_0, x_1.

The length ℓ of the body in reference space given through (22c) can be expressed in terms of force σ as

$$\ell = \bar{\ell}(\sigma) := \frac{\sigma_{\max} - \sigma}{K\widehat{\lambda}(\sigma)}, \tag{27}$$ eq:ls

for all $\sigma < \sigma_{\max}$, where the function $\widehat{\lambda}(\sigma)$ is the inverse of the force-stretch relation $\sigma = W'(\lambda)$ introduced in eq. (10). In view of (11)-(12), this shows that

$$\bar{\ell}\,'(\sigma) < 0, \quad \bar{\ell}(\sigma) \to +\infty \text{ as } \sigma \to -\infty, \quad \bar{\ell}(\sigma) \to 0^+ \text{ as } \sigma \to \sigma_{\max}^-. \tag{28}$$ eq:lsprop

The function $\bar{\sigma}(\ell)$ that is inverse to $\bar{\ell}(\sigma)$ obeys

$$\begin{aligned} &\bar{\ell}(\bar{\sigma}(\ell)) = \ell && \bar{\sigma}(\ell) \to \sigma_{\max}^- \quad \text{as} \quad \ell \to 0^+, \\ &\bar{\sigma}'(\ell) < 0 && \bar{\sigma}(\ell) \to -\infty \quad \text{as} \quad \ell \to +\infty\,. \end{aligned} \tag{29}$$ eq:sl

From equations (27)-(29) we can appreciate how growth, i.e. a change of the length of the bar ℓ in the reference configuration, affects force and stretch at equilibrium. A decrease in length ℓ in (27) produces an increase in stretch λ and in force σ till, eventually, ℓ goes to zero, stretch λ to infinity and the force to its maximum value $\sigma_{\max}$. Conversely, an increase in material length ℓ decreases both stretch and force. An indefinite increase of ℓ leads the force towards infinite compressive values and stretch towards zero.

I tried rephrasing this paragraph.

ss:DAEdiff

5.2. *Diffusion*

eq:dsol

The solution of the system of equations (3) yields

$$\begin{cases} \mu(y,t) = M_1 \dfrac{y - y_0}{y_1 - y_0} + \mu_0 \dfrac{y_1 - y}{y_1 - y_0}, & \forall\ y_0(t) \le y \le y_1(t) \qquad (30a) \quad \texttt{eq:dsol1} \\ h(y,t) = -m \dfrac{M_1 - \mu_0}{y_1 - y_0} \qquad (30b) \quad \texttt{eq:dsol2} \\ \mu_0 = M_1 + \dfrac{\varrho}{m}\,(y_1 - y_0)\,\dot{x}_0 \qquad (30c) \quad \texttt{eq:dsol3} \end{cases}$$

and we recall that $y_1 - y_0 = \lambda\ell$. Using (22c) and (25) one can express μ_0 in terms of the force σ,

$$\mu_0 = M_1 + \frac{\varrho}{Km}(\sigma_{\max} - \sigma)\,\dot{x}_0\,. \tag{31}$$ eq:mu0s

Observe that (31) can be used to eliminate the unknown chemical potential μ_0 from the other equations where its appears, namely (6a), (30a) and (30b).

Finally we note that if x_0 and x_1 are known, then as noted previously y_1 can be determined from (21), (25) and (26), $y_0 = Y_0$ being of course known. If in addition $\dot{x}_0$ is known then the chemical potential and flux fields are fully determined through (30).

ss:DAEaccr

5.3. Accretion

Using (31) and noting that $\sigma_0(t) = \sigma_1(t) = \sigma(t)$, we rewrite the pair of kinetic equations (6) as

eq:asub

$$\begin{cases} \dot{x}_0(t) = -\dfrac{1}{B_0}\dfrac{\varrho(M_1 - M_{B,0}) + W^*(\sigma(t))}{1 + \frac{\varrho^2}{mB_0K}(\sigma_{\max} - \sigma)}, & \text{(32a)} \quad \texttt{eq:asub1} \\ \dot{x}_1(t) = \dfrac{1}{B_1}\left(\varrho(M_1 - M_{B,1}) + W^*(\sigma(t))\right) & \text{(32b)} \quad \texttt{eq:asub2} \end{cases}$$

We now introduce forces $\sigma_{\alpha 0}$, $\sigma_{\alpha 1}$ exploiting the bijectivity of $W^*(\sigma)$ in $\mathbb{R}$

$$\sigma_{\alpha 0} \,:\, -W^*(\sigma_{\alpha 0}) = \varrho(M_1 - M_{B,0})\,, \quad \sigma_{\alpha 1} \,:\, -W^*(\sigma_{\alpha 1}) = \varrho(M_1 - M_{B,1})\,. \tag{33}$$ eq:salpha

Furthermore let the forces $\Delta\sigma$, σ_{asym} be defined by

$$\Delta\sigma \coloneqq \sigma_{\text{asym}} - \sigma_{\max} \coloneqq \frac{mB_0K}{\varrho^2} > 0\,. \tag{34}$$ eq:sasym

eq:afin

This allow us to write

$$\begin{cases} \dot{x}_0(t) = R_0(\sigma) \coloneqq -\dfrac{\Delta\sigma}{B_0}\,\dfrac{W^*(\sigma(t)) - W^*(\sigma_{\alpha 0})}{\sigma_{\text{asym}} - \sigma}, & \text{(35a)} \quad \texttt{eq:afin1} \\ \dot{x}_1(t) = R_1(\sigma) \coloneqq \dfrac{1}{B_1}\,\left(W^*(\sigma(t)) - W^*(\sigma_{\alpha 1})\right) & \text{(35b)} \quad \texttt{eq:afin2} \end{cases}$$

for the accretion rates $\dot{x}_0(t)$, $\dot{x}_1(t)$ as functions $R_0(\sigma)$ and $R_1(\sigma)$ of the force, respectively.

Notice that $\sigma_{\alpha 0}$ and $\sigma_{\alpha 1}$ represent the values of force for which the accretion rates $\dot{x}_0(t)$, $\dot{x}_1(t)$ are zero. Since the chemical potential of the solvent bath M_1 can be varied, according to their definitions (33), the values of $\sigma_{\alpha 0}$ and $\sigma_{\alpha 1}$ may also be varied, but not independently. In addition, for the admissible values (24) of the force σ smaller than $\sigma_{\max}$, relation (34) and the monotonicity (14a) of $W^*(\sigma)$ tell us that

$$R_0(\sigma) \lessgtr 0 \;\text{ for } \sigma \gtrless \sigma_{\alpha 0} \text{ and } \sigma < \sigma_{\max}\,, \quad R_1(\sigma) \gtrless 0 \;\text{ for } \sigma \lessgtr \sigma_{\alpha 1}\,, \tag{36}$$ eq:R>0

underscoring in particular that $\sigma_{\alpha 0}$ and $\sigma_{\alpha 1}$ are the unique zeros of $R_0(\sigma)$ and $R_1(\sigma)$ respectively.

For $R_1(\sigma)$ we can easily infer its properties from those of W^*: it is a convex, monotonically increasing function whose image is all $\mathbb{R}$ and whose derivative tends to 0^+ for $\sigma \to -\infty$ and to $+\infty$ for $\sigma \to +\infty$.

Of $R_0(\sigma)$ we know that is tends to $-\infty$ as it approaches $\sigma_{\rm asym}$ from below. Using l'Hopital's rule we also deduce that $R_0(\sigma)$ tends to zero as $\sigma \to -\infty$. Looking at the first derivative of $R_0(\sigma)$,

$$R_0'(\sigma) = -\frac{\Delta\sigma}{B_0}\,\frac{W^*(\sigma) - W^*(\sigma_{\alpha 0}) + W^{*\,\prime}(\sigma)(\sigma_{\rm asym} - \sigma)}{(\sigma_{\rm asym} - \sigma)^2}\,, \tag{37}$$

eq:R0'

we observe that it is strictly negative when conditions $\sigma > \sigma_{\alpha 0}$ and $\sigma < \sigma_{\rm asym}$ are satisfied. Instead, R_0 is not monotonic for $\sigma < \sigma_{\alpha 0} < \sigma_{\rm asym}$, since its derivative has opposite signs at the two ends of that interval.

ss:DAEeq

5.4. Differential algebraic equation

The model under consideration reduces to the following differential algebraic equation

eq:lsdae

$$\begin{cases} \dot\ell = R_1(\sigma) - R_0(\sigma) \\ \quad = \dfrac{1}{B_1}\,(W^*(\sigma) - W^*(\sigma_{\alpha 1})) + \dfrac{\Delta\sigma}{B_0}\,\dfrac{W^*(\sigma) - W^*(\sigma_{\alpha 0})}{\sigma_{\rm asym} - \sigma}, & \text{(38a)} \quad \texttt{eq:lsdae1} \\ \ell = \bar\ell(\sigma) = \dfrac{\sigma_{\max} - \sigma}{K\; W^{*\,\prime}(\sigma)} & \text{(38b)} \quad \texttt{eq:lsdae2} \end{cases}$$

in which $\ell(t)$ and $\sigma(t)$ are sought under initial conditions, see (7),

$$\ell(0) = x_{10} - x_{00}, \quad \sigma(0) = W'\left(\frac{Y_{10} - Y_0}{x_{10} - x_{00}}\right)\,, \tag{39}$$

eq:lsinit

and under the constraint $\ell > 0$ which is equivalent to $\sigma < \sigma_{\max}$.

sec:TM

6. Existence and stability of treadmilling solutions

In a so-called treadmilling solution the length $\ell = \ell_{\rm TM}$ of the bar in the reference configuration does not vary with time: $\dot\ell = 0$, and this corresponds to values $\sigma_{\rm TM}$ of the force for which $R_0(\sigma_{\rm TM}) = R_1(\sigma_{\rm TM})$.

Relevant to the ensuing discussion is the condition

$$R_1(\sigma_{\max}) > R_0(\sigma_{\max})\,, \tag{40}$$

eq:R1>R0

which expresses the requirement that at the limit $\ell \to 0$ and $\sigma \to \sigma_{\max}$, accretion prevails on ablation.

It is possible to formulate (40) in terms of forces, introducing the force σ_β such that

$$W^*(\sigma_\beta) = \frac{1}{1+\beta}W^*(\sigma_{\alpha 0}) + \frac{\beta}{1+\beta}W^*(\sigma_{\alpha 1})\,, \quad \text{with} \quad \beta = \frac{B_0}{B_1} > 0\,. \tag{41}$$

eq:sb

From the monotonicity of W^*, it is clear that the value of σ_β is always in between the values $\sigma_{\alpha 0}$ and $\sigma_{\alpha 1}$ defined in (33).

Force σ_β has the property that condition

$$\sigma_\beta < \sigma_{\max} \tag{42}$$

eq:sb<smax

is equivalent to (40).

ss:TMstab

6.1. *Stability of treadmilling states*

We start by discussing the condition of stability of a treadmilling solution, assuming there exists one, by perturbing a treadmilling state characterized by force $\sigma_{\rm TM}$ and length $\ell_{\rm TM} = \bar{\ell}(\sigma_{\rm TM})$ according to (38b).

The perturbation of equation (10), $\lambda = \widehat{\lambda}(\sigma)$, yields

$$\delta\lambda = \widehat{\lambda}'(\sigma_{\rm TM})\delta\sigma$$

Operating analogously on equation (22c), $K\lambda\ell = \sigma_{\max} - \sigma$, gives

$$K\widehat{\lambda}(\sigma_{\rm TM})\delta\ell + K\ell_{\rm TM}\delta\lambda = -\delta\sigma$$

Combining the two preceding equations provides a relation between the perturbations $\delta\ell$ and $\delta\sigma$,

$$K\widehat{\lambda}(\sigma_{\rm TM})\,\delta\ell + \Big(K\ell_{\rm TM}\widehat{\lambda}'(\sigma_{\rm TM}) + 1\Big)\;\delta\sigma = 0. \tag{43}$$

eq:psell

From the expression (38a) of $\dot{\ell}(\sigma)$ we obtain

$$\delta\dot{\ell} = (R_1'(\sigma_{\rm TM}) - R_0'(\sigma_{\rm TM}))\;\delta\sigma.$$

Combining this with (43) yields

$$\delta\dot{\ell} = -F(\sigma_{\rm TM})\delta\ell \qquad \text{where} \quad F(\sigma_{\rm TM}) = \frac{R_1'(\sigma_{\rm TM}) - R_0'(\sigma_{\rm TM})}{K\ell_{\rm TM}\widehat{\lambda}'(\sigma_{\rm TM}) + 1}\,K\widehat{\lambda}(\sigma_{\rm TM}).$$

The treadmilling solution is stable if the ordinary differential equation $\delta\dot{\ell}(t) = -F(\sigma_{\rm TM})\delta\ell(t)$ has exponentially decaying solutions[1], and this occurs if and only if $F(\sigma_{\rm TM}) > 0$. Since $\widehat{\lambda}(\sigma_{\rm TM}) > 0$, $\ell_{\rm TM} > 0$ and $\widehat{\lambda}'(\sigma_{\rm TM}) > 0$ it follows that the treadmilling solution is stable if and only if

$$R_1'(\sigma_{\rm TM}) > R_0'(\sigma_{\rm TM}). \tag{44}$$

eq:TMstable

It is interesting to use the monotonic relation (27) between the force σ and the referential length ℓ to plot the evolution of the system in the neighborhood of a stable treadmilling solution on the $\ell, \dot{\ell}$-plane. Given that $\ell = \bar{\ell}(\sigma)$ is a monotonically decreasing function, and using (44),(38a),(29), the slope of $\dot{\ell}(\ell)$ is found to be negative close to a stable treadmilling.

This is shown schematically in Figure 3. Observe how, if $\ell > \ell_{\rm TM}$ at some time then $\dot{\ell} < 0$ and so $\ell(t)$ will decrease until it reaches the treadmilling value $\ell_{\rm TM}$. Likewise if $\ell < \ell_{\rm TM}$, $\ell(t)$ will increase to $\ell_{\rm TM}$.

[1] If $\delta\ell(t)$ vanishes exponentially then so do the perturbations of the various other quantities.

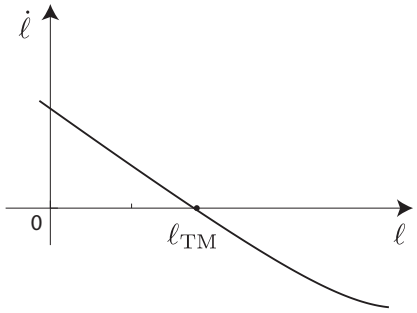

Figure 3: Graph of $\dot{\ell} = \dot{x}_1 - \dot{x}_0 = R_1(\sigma(\ell)) - R_0(\sigma(\ell))$ versus ℓ where $\sigma(\ell)$ is given through (22c). fig:ell

ss:TMexist

6.2. *Existence of treadmilling solutions*

sss:TM0<1

6.2.1. *$M_{B,0}$ smaller than $M_{B,1}$*

We discuss first the case that is more relevant with regard to the applications (Tomassetti et al., 2016; Abi-Akl et al., 2019) and experiments (Cameron et al., 1999; Noireaux et al., 2000; van der Gucht et al., 2005; Bieling et al., 2016) this model is aiming to analyze, namely the situation in which at treadmilling accretion takes place at the fixed end Y_0, and ablation at the free end y_1.

We assume

$$M_{B,0} < M_{B,1} \tag{45}$$ eq:MB0<MB1

that is the ATP-actin to be in Y_0 and the hydrolyzed ADP-actin in y_1. From the definition (33) and from the monotonicity (14a) of W^*, it follows that

$$\sigma_{\alpha 0} < \sigma_{\alpha 1}\,. \tag{46}$$ eq:sa0<sa1

Under the above provision, it is possible to prove that,

Proposition 1 (Existence and uniqueness)**.** *$\sigma_\beta < \sigma_{\max}$ is a necessary and sufficient condition for the existence and uniqueness of a treadmilling solution. Such solution is globally stable.*

Proof. Assume $\sigma_\beta < \sigma_{\max}$ holds. Then $\sigma_{\alpha 0} < \sigma_{\max}$ given that $\sigma_{\alpha 0} < \sigma_\beta < \sigma_{\alpha 1}$. Moreover, as observed in section 5.3, in the interval $\sigma_{\alpha 0} < \sigma < \sigma_{\max}$

- $R_0(\sigma)$ is negative,
- $R_0(\sigma)$ is monotonically decreasing,
- $R_1(\sigma)$ is monotonically increasing,
- $R_1(\sigma_{\alpha 0}) < R_0(\sigma_{\alpha 0}) = 0$,
- $R_1(\sigma_{\max}) > R_0(\sigma_{\max})$.

Given the continuity of $R_0(\sigma)$ and $R_1(\sigma)$, the two functions certainly intersect between $\sigma_{\alpha 0}$ and $\sigma_{\max}$ because their difference has opposite values at the extremes of the interval. Uniqueness follows from monotonicity. The negative sign of R_0 implies that both functions are negative in the intersection σ_{TM}, therefore treadmilling lies in the interval $\sigma_{\alpha 0} < \sigma_{\mathrm{TM}} < \min(\sigma_{\alpha 1}, \sigma_{\max})$. From monotonicity we also additionally infer that condition (44) is met and that the unique treadmilling solution is always stable. In fact it is globally stable because the rate $\dot{\ell} = R_1(\sigma) - R_0(\sigma)$ is always negative for all $\sigma < \sigma_{\mathrm{TM}}$, i.e. for $\ell > \ell_{\mathrm{TM}}$, and viceversa $\dot{\ell} > 0$ for $\sigma > \sigma_{\mathrm{TM}}$.

Conversely assume $\sigma_\beta \geq \sigma_{\max}$. The case $\sigma_\beta = \sigma_{\max}$ corresponds to a non admissible treadmilling solution in which the bar has zero reference length ℓ and force equal to $\sigma_{\max}$.

Consider the case $\sigma_\beta > \sigma_{\max}$. According to (36), there is no intersection in the interval $\sigma < \min(\sigma_{\alpha 0}, \sigma_{\max}) < \sigma_{\alpha 1}$, because $R_0(\sigma)$ is positive and $R_1(\sigma)$ negative. This ends the proof if $\sigma_{\alpha 0} \geq \sigma_{\max}$. If $\sigma_{\alpha 0} < \sigma_{\max}$, we consider the interval $\sigma_{\alpha 0} \leq \sigma < \sigma_{\max}$: both $R_0(\sigma)$ and $R_1(\sigma)$ are monotonic and R_0 is above R_1 at both ends of the interval. Hence any intersection is excluded also in this case.

□

An example of functions R_0 and R_1 in the case $\sigma_{\alpha 0} < \sigma_{\alpha 1}$ is given in Figure 4. There we see that at $\sigma = \sigma_{\max}$, condition (40), is met and therefore a

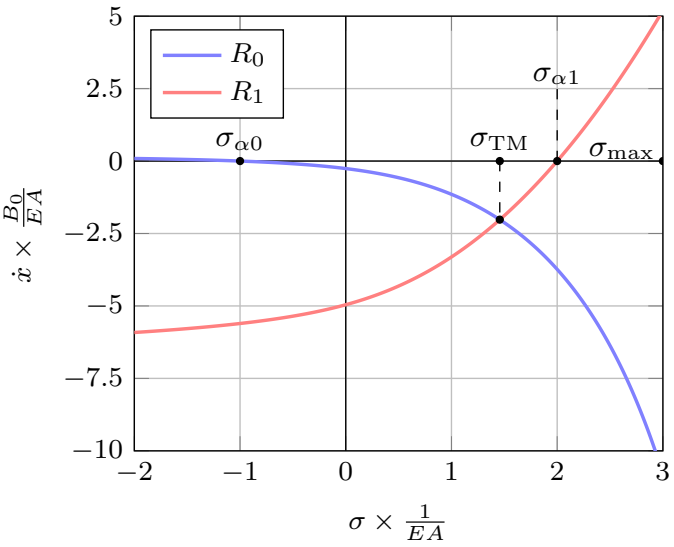

Figure 4: Example of treadmilling solution obtained using $W^*(\sigma)$ from eq. (16) with parameters $\sigma_{\mathrm{asym}} = 5EA$, $\sigma_{\max} = 3EA$, $\sigma_{\alpha 0} = -EA$, $\sigma_{\alpha 1} = 2EA$, $\beta = 1.0$. fig:tm1

unique, globally stable, treadmilling solution exists. This result corroborates

the globally stable equilibrium observed numerically by Abi-Akl et al. (2019) in a similar setting.

Starting from the computed value of the force σ_{TM} it is possible to reconstruct the whole system at treadmilling. The corresponding stretch λ_{TM} is given by $\lambda_{\mathrm{TM}} = \widehat{\lambda}(\sigma_{\mathrm{TM}})$; the growth rates at the two ends are $\dot{x}_0^{\mathrm{TM}} = \dot{x}_1^{\mathrm{TM}} = R_0(\sigma_{\mathrm{TM}}) = R_1(\sigma_{\mathrm{TM}})$; the length of the body in reference space is $\ell_{\mathrm{TM}} = \bar{\ell}(\sigma_{\mathrm{TM}})$; the length of the body in physical space is $\lambda_{\mathrm{TM}}\ell_{\mathrm{TM}}$; and the chemical potential at the growing end is $\mu_0^{\mathrm{TM}} = M_1 + \varrho(\sigma_{\max} - \sigma_{\mathrm{TM}})\dot{x}_0^{\mathrm{TM}}/(Km)$.

If, differently from the situation represented in Figure 4, the value of $\sigma_{\max}$ is on the left of the intersection σ_{TM} of R_0 and R_1, then there is no treadmilling solution. According to (38a), we have $\dot{\ell}$ negative everywhere in the admissible domain, so starting from any finite material length $x_{10} - x_{00}$, the rod progressively loses all of its monomers till it reaches $\ell = 0$ and $\sigma = \sigma_{\max}$.

It is interesting to represent the evolution in space, see Figure 5, and time, see Figure 6, of the energy of a mole of actin as it undergoes treadmilling.

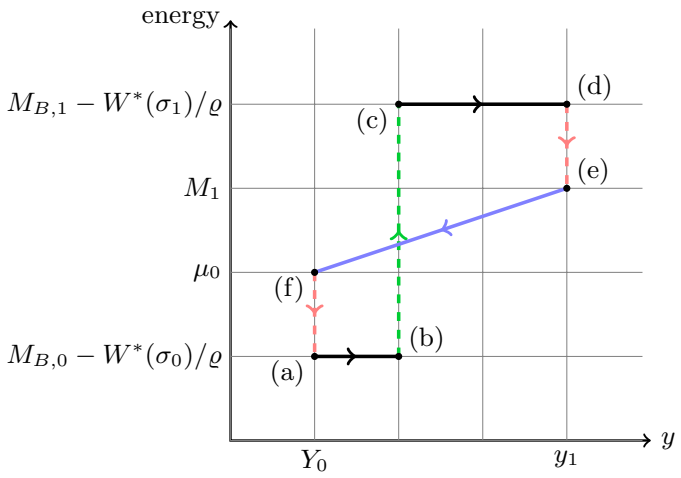

Figure 5: Evolution in space of the energy of a mole of actin as it undergoes treadmilling. Blue represents diffusion, red accretion/ablation and green ATP-hydrolysis.

fig:tm-eny

In Figure 5, ATP-actin accretes in Y_0 following the red dashed line and losing energy in the process. Then it hydrolyzes after some time to ADP-actin following the green segment and reaching a higher energy level. Ablation, again indicated by a red dashed line, takes place in y_1 and is accompanied by energy loss. The mole of actin then diffuses back to Y_0 along the blue line and the process starts again (note: when does ADP actin becomes ATP actin again? and is there an energy jump in the process?). The same evolution is represented in Figure 6, with the difference that, consistently with the model assumptions, the instantaneous diffusion segment is vertical.

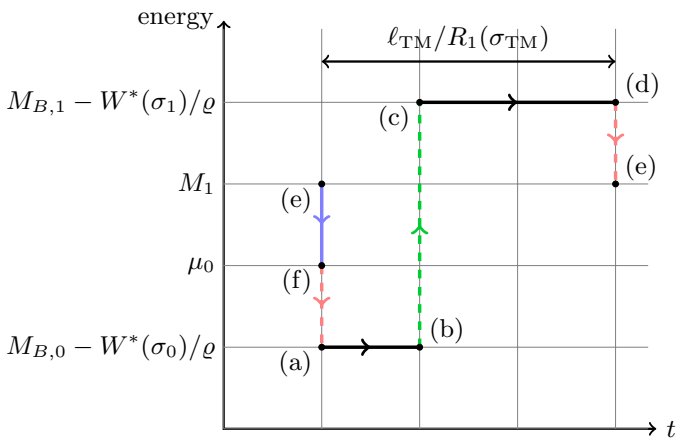

Figure 6: Evolution in time of the energy of a mole of actin as it undergoes treadmilling. Blue represents diffusion, red accretion/ablation and green ATP-hydrolysis. fig:tment

sss:TM0>1

6.2.2. $M_{B,0}$ larger than $M_{B,1}$

We now discuss the case in which at treadmilling accretion takes place at the free end y_1, and ablation at the fixed end Y_0. This situation could resemble the experimental set-ups of Parekh et al. (2005) and Chaudhuri et al. (2007), though treadmilling was not investigated there.

We assume

$$M_{B,0} > M_{B,1} \tag{47}$$ eq:MB0>MB1

that is the ATP-actin to be in y_1 and the hydrolyzed ADP-actin in Y_0. From the definition (33) and from the monotonicity (14a) of W^*, it follows that

$$\sigma_{\alpha 0} > \sigma_{\alpha 1} \tag{48}$$ eq:sa0>sa1

Under the above condition, it is possible to prove that,

Proposition 2 (Existence)**.** *$\sigma_\beta < \sigma_{\max}$ is a sufficient condition for the existence of a treadmilling solution.*

Proof. Assume $\sigma_\beta < \sigma_{\max}$ holds. Then $\sigma_{\alpha 1} < \sigma_{\max}$ given that $\sigma_{\alpha 1} < \sigma_\beta < \sigma_{\alpha 0}$. Moreover, as observed in section 5.3, in the interval $\sigma_{\alpha 1} < \sigma < \sigma_{\max}$

- $R_1(\sigma)$ is positive,
- $R_0(\sigma_{\alpha 1}) > R_1(\sigma_{\alpha 1}) = 0$,
- $R_1(\sigma_{\max}) > R_0(\sigma_{\max})$.

Given the continuity of $R_0(\sigma)$ and $R_1(\sigma)$, the two functions certainly intersect at least once between $\sigma_{\alpha 1}$ and $\sigma_{\max}$ because their difference has opposite values at the extremes of the interval. Positiveness of $R_1(\sigma)$, implies that both $R_0(\sigma_{\rm TM})$

and $R_1(\sigma_{\rm TM})$ are positive, therefore treadmilling states may only exist in the interval $\sigma_{\alpha 1} < \sigma_{\rm TM} < \min(\sigma_{\alpha 0}, \sigma_{\rm max})$. The solution is not unique because R_0 is not necessarily monotonic for $\sigma < \sigma_{\alpha 0}$.

□

An example of functions R_0 and R_1 in the case $\sigma_{\alpha 0} > \sigma_{\alpha 1}$ is given in Figure 7. The picture is drawn for a case in which $\sigma_{\rm asym} < \sigma_{\alpha 0}$ and in which,

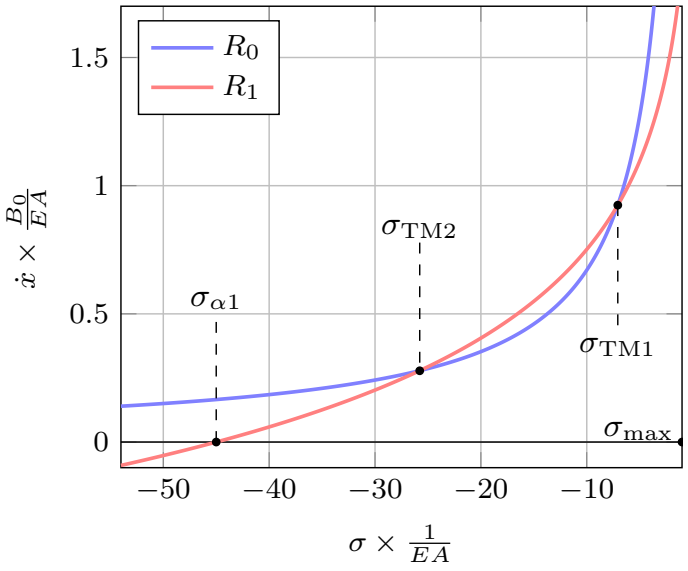

Figure 7: Example of treadmilling solution obtained using $W^*(\sigma)$ from eq. (16) with parameters $\sigma_{\rm asym} = 0$, $\sigma_{\rm max} = -EA$, $\sigma_{\alpha 0} = 2EA$, $\sigma_{\alpha 1} = -45EA$, $\beta = 1.0$. (I haven't so far been able to find multiple intersections in the case $\sigma_{\alpha 0} < \sigma_{\rm asym}$)

fig:tm2

correspondingly, both R_0 and R_1 are monotonically increasing in the domain $\sigma < \sigma_{\rm max}$. Notice that multiple treadmilling solutions exist despite conditions (40), (42) not being met, because in the current case $\sigma_{\alpha 1} < \sigma_{\alpha 0}$ such conditions are sufficient but not necessary for the existence of treadmilling solutions. According to the local stability criterion (44), the first treadmilling state characterized by force $\sigma_{\rm TM1}$ is unstable while the other at force $\sigma_{\rm TM2}$ is stable. The basin of attraction of the latter solution is any initial condition corresponding to a force $\sigma < \sigma_{\rm TM1}$. Bars with initial conditions having $\ell < \ell_{\rm TM1}$, i.e. $\sigma > \sigma_{\rm TM1}$, have negative $\dot{\ell}$ and therefore progressively loose all of their monomers till they reach zero length and force $\sigma_{\rm max}$.

sec:end

7. Conclusions

We presented a one-dimensional, self-contained growth model for an actin bar fixed at one end and elastically constrained at the other. The model en-

compasses diffusion in a solvent surrounding or permeating the bar as well as growth conditions at the ends. The nonlinear elastic material properties of actin are specified through general requirements on its strain energy density, the main one being convexity.

Treadmilling states were investigated in which the length of the bar remains constant while accreting actin monomers at one end and ablating them at the opposite end at equal rates. The treadmilling state in which monomers accrete at the fixed end is found to be globally stable. Multiple treadmilling states in which monomers ablate at the fixed end are instead possible.

Conditions for existence and stability of treadmilling states were condensed in relatively simple formulas which can be useful to appreciate the influence of different parameters and explain the results of more complex models. For instance, global stability of treamilling states accreting monomers at the fixed end can provide additional explanation to the numerical findings made by Abi-Akl et al. (2019) in a similar setting.

Further refinements of the model could also be relevant for applications, especially experimental ones: accounting for the density and stiffness increase of actin under higher external load and developing analytical relationships between growth velocity and applied force are two of them. Finally, extension of the present work to the stability of two dimensional treadmilling states previously studied in Tomassetti et al. (2016) is planned.

Acknowledgements

R.A. and E.P. gratefully acknowledge the support of the MIT-FVG Seed Fund. E.P. thankfully acknowledges as well the support of the Italian National Group of Mathematical Physics (GNFM-INdAM).

References

AbeyaratneKnowles1990 Abeyaratne, R., Knowles, J.K., 1990. On the driving traction acting on a surface of strain discontinuity in a continuum. Journal of the Mechanics and Physics of Solids 38, 345–360. doi:10.1016/0022-5096(90)90003-M.

AbeyaratneKnowles1997 Abeyaratne, R., Knowles, J.K., 1997. A note on the driving traction acting on a propagating interface: Adiabatic and non-adiabatic processes of a continuum. Journal of Applied Mechanics 67, 829–830. doi:10.1115/1.1308577.

Abi-AklAbeyaratne2019 Abi-Akl, R., Abeyaratne, R., Cohen, T., 2019. Kinetics of surface growth with coupled diffusion and the emergence of a universal growth path. Proceedings of the Royal Society A: Mathematical, Physical and Engineering Sciences 475, 20180465. doi:10.1098/rspa.2018.0465.

AlbertsJohnson2015 Alberts, B., Johnson, A., Lewis, J., Morgan, D., Raff, M., 2015. Molecular Biology of the Cell. 6 ed., Garland Science.

BacigalupoGambarotta:2012 Bacigalupo, A., Gambarotta, L., 2012. Effects of layered accretion on the mechanics of masonry structures. Mechanics Based Design of Structures and Machines 40, 163–184. doi:10.1080/15397734.2011.628622.

BielingLi2016 Bieling, P., Li, T.D., Weichsel, J., McGorty, R., Jreij, P., Huang, B., Fletcher, D., Mullins, R.D., 2016. Force feedback controls motor activity and mechanical properties of self-assembling branched actin networks. Cell 164, 115–127. doi:10.1016/j.cell.2015.11.057.

BindschadlerOsborn2004 Bindschadler, M., Osborn, E.A., Dewey, C.F., McGrath, J.L., 2004. A mechanistic model of the actin cycle. Biophysical Journal 86, 2720–2739. doi:10.1016/S0006-3495(04)74326-X.

BuylMikhailov2013 de Buyl, P., Mikhailov, A.S., Kapral, R., 2013. Self-propulsion through symmetry breaking. EPL (Europhysics Letters) 103, 60009. doi:10.1209/0295-5075/103/60009.

CameronFooter1999 Cameron, L.A., Footer, M.J., van Oudenaarden, A., Theriot, J.A., 1999. Motility of acta protein-coated microspheres driven by actin polymerization. Proc Natl Acad Sci USA 96, 4908–4913. doi:10.1073/pnas.96.9.4908.

CardamoneLaio2011 Cardamone, L., Laio, A., Torre, V., Shahapure, R., DeSimone, A., 2011. Cytoskeletal actin networks in motile cells are critically self-organized systems synchronized by mechanical interactions. Proc Natl Acad Sci USA 108, 13978–13983. doi:10.1073/pnas.1100549108.

ChaudhuriParekh2007 Chaudhuri, O., Parekh, S.H., Fletcher, D.A., 2007. Reversible stress softening of actin networks. Nature 445, 295–298. doi:10.1038/nature05459.

CiarlettaPreziosi2013 Ciarletta, P., Preziosi, L., Maugin, G.A., 2013. Mechanobiology of interfacial growth. Journal of the Mechanics and Physics of Solids 61, 852–872. doi:10.1016/j.jmps.2012.10.011.

stein-KeshetErmentrout2000 Edelstein-Keshet, L., Ermentrout, G.B., 2000. Models for spatial polymerization dynamics of rod-like polymers. Journal of Mathematical Biology 40, 64–96. doi:10.1007/s002850050005.

GanghofferGoda2018 Ganghoffer, J.F., Goda, I., 2018. A combined accretion and surface growth model in the framework of irreversible thermodynamics. International Journal of Engineering Science 127, 53–79. doi:10.1016/j.ijengsci.2018.02.006.

Goriely:2017 Goriely, A., 2017. The Mathematics and Mechanics of Biological Growth. volume 45 of *Interdisciplinary Applied Mathematics*. 1 ed., Springer. doi:10.1007/978-0-387-87710-5.

GuchtPaluch2005 van der Gucht, J., Paluch, E., Plastino, J., Sykes, C., 2005. Stress release drives symmetry breaking for actin-based movement. Proc Natl Acad Sci USA 102, 7847. doi:10.1073/pnas.0502121102.

JohnPeyla2008 John, K., Peyla, P., Kassner, K., Prost, J., Misbah, C., 2008. Nonlinear study of symmetry breaking in actin gels: Implications for cellular motility. Physical Review Letters 100, 068101. doi:10.1103/PhysRevLett.100.068101.

NoireauxGolsteyn:2000 Noireaux, V., Golsteyn, R.M., Friederich, E., Prost, J., Antony, C., Louvard, D., Sykes, C., 2000. Growing an actin gel on spherical surfaces. Biophysical Journal 78, 1643–1654. doi:10.1016/S0006-3495(00)76716-6.

ParekhChaudhuri2005 Parekh, S.H., Chaudhuri, O., Theriot, J.A., Fletcher, D.A., 2005. Loading history determines the velocity of actin-network growth. Nature Cell Biology 7, 1219–1223. doi:10.1038/ncb1336.

ProstJuelicher2015 Prost, J., Jülicher, F., Joanny, J.F., 2015. Active gel physics. Nature Physics 11, 111–117. doi:10.1038/nphys3224.

ProstJoanny2008 Prost, J., Joanny, J.F., Lenz, P., Sykes, C., 2008. The physics of listeria propulsion, in: Lenz, P. (Ed.), Cell Motility. Springer New York, New York, NY. Biological and Medical Physics, Biomedical Engineering. chapter 1, pp. 1–30. doi:10.1007/978-0-387-73050-9_1.

SkalakDasgupta1982 Skalak, R., Dasgupta, G., Moss, M., Otten, E., Dullemeijer, P., Vilmann, H., 1982. Analytical description of growth. Journal of Theoretical Biology 94, 555–577. doi:10.1016/0022-5193(82)90301-0.

SkalakFarrow1997 Skalak, R., Farrow, D.A., Hoger, A., 1997. Kinematics of surface growth. Journal of Mathematical Biology 35, 869–907. doi:10.1007/s002850050081.

Theriot2000 Theriot, J.A., 2000. The polymerization motor. Traffic 1, 19–28. doi:10.1034/j.1600-0854.2000.010104.x.

TomassettiCohen:2016 Tomassetti, G., Cohen, T., Abeyaratne, R., 2016. Steady accretion of an elastic body on a hard spherical surface and the notion of a four-dimensional reference space. Journal of the Mechanics and Physics of Solids 96, 333–352. doi:10.1016/j.jmps.2016.05.015.

Zimmermann2014 Zimmermann, J., 2014. Modeling the lamellipodium of motile cells. Ph.D. thesis. Humboldt-Universität zu Berlin, Mathematisch-Naturwissenschaftliche Fakultät I. doi:10.18452/16871.

ZurloTruskinovsky2017 Zurlo, G., Truskinovsky, L., 2017. Printing non-euclidean solids. Physical Review Letters 119, 048001. doi:10.1103/PhysRevLett.119.048001.

ZurloTruskinovsky2018 Zurlo, G., Truskinovsky, L., 2018. Inelastic surface growth. Mechanics Research Communications 93, 174–179. doi:10.1016/j.mechrescom.2018.01.007.